Electronic Supplementary Material (ESI) for ChemComm.
This journal is © The Royal Society of Chemistry 2023

Supporting Information

A TCF-based fluorescent probe to determine nitroreductase (NTR) activity for a broad-spectrum of bacterial species

Kai-Cheng Yan,[a,c] Jordan E. Gardiner,[a] Adam C. Sedgwick,[b] Naing Thet,[a] Rachel A. Heylen,[a] Tony D. James*,[a,d] A. Toby A. Jenkins*[a] and Xiao-Peng He*[c,e]

[a]*Department of Chemistry, University of Bath, Bath, BA2 7AY, U.K.*
[b]*Chemistry Research Laboratory, University of Oxford, Mansfield Road, OX1 3TA, UK.*
[c]*Key Laboratory for Advanced Materials and Joint International Research Laboratory of Precision Chemistry and Molecular Engineering, Feringa Nobel Prize Scientist Joint Research Center, School of Chemistry and Molecular Engineering, East China University of Science and Technology, 130 Meilong Rd., Shanghai 200237, China.*
[d]*School of Chemistry and Chemical Engineering, Henan Normal University, Xinxiang 453007, China. National Center for Liver Cancer, The International Cooperation Laboratory on Signal Transduction, Eastern Hepatobiliary Surgery Hospital, the Second Military Medical University, Shanghai 200433, China.*
[e]*National Center for Liver Cancer, The International Cooperation Laboratory on Signal Transduction, Eastern Hepatobiliary Surgery Hospital, the Second Military Medical University, Shanghai 200433, China.*

*Corresponding authors.
t.d.james@bath.ac.uk (TDJ)
a.t.a.jenkins@bath.ac.uk (ATAJ)
xphe@ecust.edu.cn (XPH)

Table of Contents

1. Experimental

General

Apart from the compounds made from chemical reaction, all the auxiliary chemicals used in the study are commercially available. Materials used in biological experiments were kindly provided by Professor Toby Jenkins, University of Bath, U.K. Thin-layer chromatography (TLC) was performed on silica gel plates and visualized by UV to track the reaction. Nuclear Magnetic Resonance (NMR) characterizations were recorded by an Agilent ProPulse 500 spectrometer. Mass Spectrum (MS) analyses were performed using an Agilent QTOF 6545 with Jetstream ESI spray source coupled to an Agilent 1260 Infinity II Quat pump HPLC with 1260 autosampler, column oven compartment and variable wavelength detector (VWD). Fluorescence emission measurements were performed on a BMG Labtech CLARIO star plate reader using Greiner Bio-One microplates (96-well, black-walled). Data were collected via the BMG Labtech Clariostar data analysis software package MARS. UV-Vis absorption measurements were performed on a Varian Cary 500 UV-Vis spectrophotometer. Fluorescence imaging was carried out on a ZEISS LSM-880 Inverted Confocal Laser Scanning Microscope equipped with 561 nm laser source, where samples were prepared on microscopy glass slides. The pH values were measured on a Hanna Instruments HI 9321 Microprocessor pH meter which was routinely calibrated using Fisher Chemicals standard buffer solutions.

Basic Patterns

Bacterial Strains. The strains used include *P. aeruginosa* PAO1, ATCC 27853, *E. coli* NCTC 10418, BW 25113, ATCC 25922, DH5α, NSM59, WPR, *S. aureus* NCTC 10788, H560, *S. dysgalactiae* NCTC 10238, NCTC 12048, *E. faecalis* JH2-2, ATCC 29212, which were kindly provided by Professor Toby Jenkins, University of Bath, U.K.

Probe Incubation & Detection. Probe **TCF-Nitro** in pH = 8.0 PBS buffer (10 μM) was co-incubated with overnight-cultured planktonic cells after washing, under shaking for 1 h or 1 d respectively at 37 °C, where the suspensions were constantly mixed. For the inhibition assay, nitroreductase (NTR) inhibitor dicoumarin was firstly treated with the cells before probe incubation, then washed out to incubate probe. Alternatively, NTR inhibitor dicoumarin was firstly treated with the cells before probe incubation. After, systems were taken to centrifugation (14000 rpm, 3 min) and the supernatants were moved to black well plates for fluorescence detection.

Colony Biofilm Model. Colony biofilms were prepared as outlined by Thet et al.[1] with some modifications. First, polycarbonate membranes were UV sterilised for 10 min on Brain-Herat Infusion Agar, before being inoculated with 30 μL Artificial Wound Fluid (AWF; 50% fetal bovine serum in 50% peptone water [0.9% sodium chloride in 0.1% peptone]). Once dry, 50 μL of sub-cultured bacteria suspension was placed on the

membrane and allowed to dry at room temperature under wind blow. The inoculated polycarbonate membranes were then placed facing down and incubated for 1 d at 37 °C. Next, biofilms were removed from the agar plate, and placed into wells with 10 μM **TCF-Nitro** in PBS buffer (pH = 8.0), before being protected from light and incubated at 37 °C for 1 h and 1 d respectively. For the inhibition assay wells, NTR inhibitor dicoumarin was firstly treated with the biofilms in the wells before probe incubation. After, the suspension was removed and centrifuged (14000 rpm, 3 min), and supernatant was subsequently placed into black well plate for fluorescence detection.

Confocal Laser-Scanning Microscopy (CLSM) Imaging. The sub-cultures were allowed to grow at 37 °C for 1 d with presence of probe, under shaking and constant mixing. Then, the systems were then taken to centrifugation (14000 rpm, 3 min), and the remaining bacteria were washed with PBS buffer before incubating with probe 10 μM **TCF-Nitro** in PBS buffer (pH = 8.0) for 1 d. For the inhibition assay wells, NTR inhibitor dicoumarin was firstly treated with the biofilms in the wells before probe incubation. Then, systems were taken to centrifugation (14000 rpm, 3 min), and the remaining bacteria were washed with PBS buffer for three times, resuspended and placed onto microscope glass slides respectively (covered with cover glass).

Fluorescence Quantum Yields. Use Rhodamine B as a reference agent to measure the fluorescent quantum yield, and determine the ultraviolet absorption and fluorescent curve of both Rhodamine B and NTR-activated **TCF-Nitro** (**TCF-OH***) at different concentrations, respectively. The following data are obtained:

□		1	2	3	4	5
Rhodamine B	UV	0.040018	0.044892	0.048779	0.050308	0.058236
	FL	1267.952	1874.349	2068.662	2495.149	2738.453
TCF-OH*	UV	0.048779	0.449091	0.449091	0.004626	0.404688
	FL	4004.958	48104.96	48104.96	622.8189	51208.82

Groups: 1 – 5 μM; 2 – 6 μM; 3 – 7.5 μM; 4 – 8 μM; 5 – 10 μM.

Based on the fluorescence quantum yield formula $\frac{F_U}{A_U}=\frac{Y_U F_S}{Y_S A_S}$, ($F_U/A_U$: the fluorescence intensity peak area and absorbance of **TCF-OH***. Fs and AS: the fluorescence intensity peak area and absorbance of rhodamine B. Yu: the fluorescence quantum yield of **TCF-OH***, Y_S: the fluorescence quantum yield of rhodamine B), respectively calculate $\frac{F_U}{A_U}$ and $\frac{F_S}{A_S}$，use formula $\frac{F_U}{A_U}=\frac{Y_U F_S}{Y_S A_S}$ to obtain curve (slope: $\frac{Y_U}{Y_S}$):

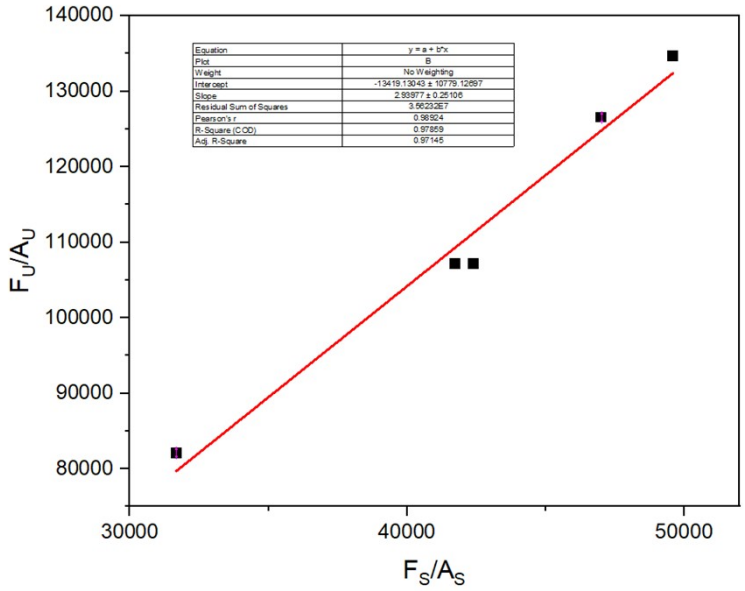

Based on the fluorescent quantum yield of Rhodamine B (0.31), and the slope of its fitting curve is 2.93, the fluorescent quantum yield of probe after activation is determined as 0.31*2.93 = 0.91.

Synthesis

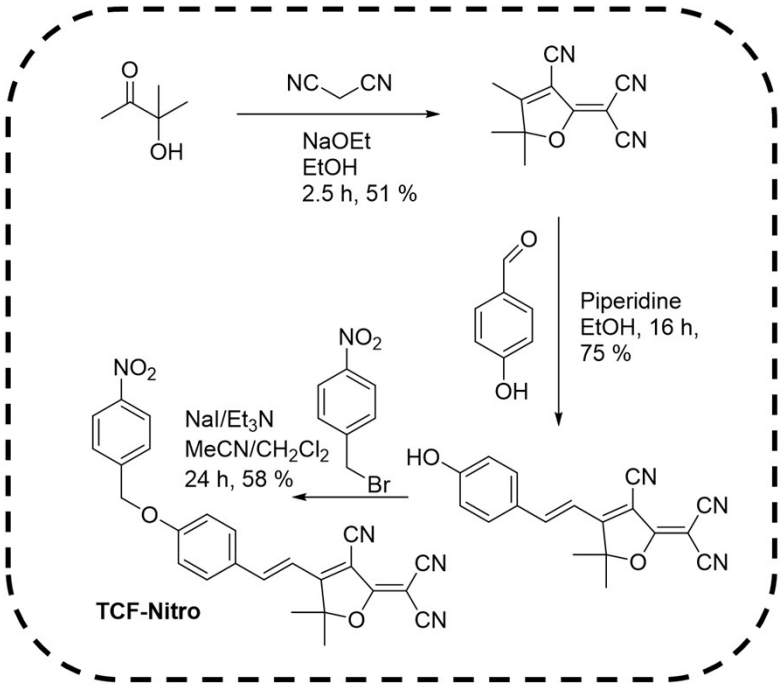

Scheme S1. Synthesis of **TCF-Nitro**.

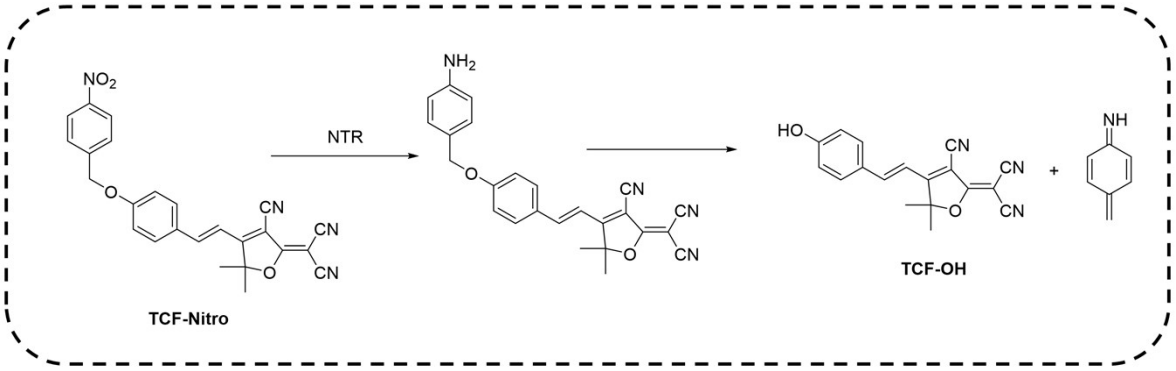

Scheme S2. Enzymatic reaction of **TCF-Nitro** to show fluorescence response.

2-(3-cyano-4,5,5-trimethylfuran-2(5H)-ylidene)malononitrile (TCF) and **(E)-2-(3-cyano-4-(4-hydroxystyryl)-5,5-dimethylfuran-2(5H)-ylidene)malononitrile (TCF-OH)** are made as outlined in the reference.[2]

2-(3-Cyano-5,5-dimethyl-4-{2-[4-(4-nitro-benzyloxy)-phenyl]-vinyl}-5H-furan-2-ylidene)-malononitrile (TCF-Nitro)

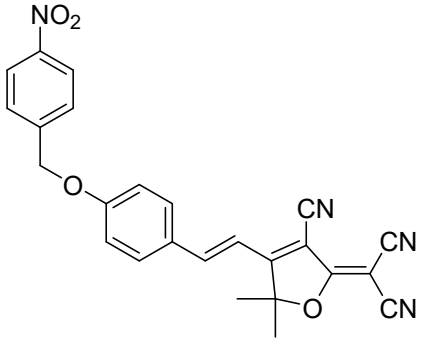

Triethylamine (260 μL) was added to a solution of **TCF-OH** (0.2 g, 0.66 mmol) in MeCN/CH_2Cl_2 (15 mL/5 mL, 3:1). Then, 4-Nitrobenzyl bromide (0.285 g,1.32 mmol) and Nal (0.01 g, 0.067 mmol) was added to the reaction upon stirring. The reaction was stirred at 60 °C under reflux for 24 h, before being concentrated *in-vacuo* to afford the crude material. The crude was purified *via* column chromatography (pure CH_2Cl_2) and the title compound was isolated (0.166 g, 0.38 mmol, 58%). The title compound was afforded as a red solid. ^{1}H NMR (500 MHz, DMSO-D_6) δ 8.27 (d, J = 8.7 Hz, 2H), 7.95 - 7.88 (m, 3H), 7.74 (d, J = 8.7 Hz, 2H), 7.18 (d, J = 8.9 Hz, 2H), 7.10 (d, J = 16.4 Hz, 1H), 5.40 (s, 2H), 1.78 (s, 6H). ^{13}C NMR (126 MHz, DMSO-D_6) δ 177.68, 176.06, 161.97, 147.85, 147.60, 144.77, 132.31, 128.85, 128.13, 124.12, 116.23, 113.65, 113.28, 112.44, 111.52, 99.68, 98.27, 68.84, 54.24, 25.67. HRMS (ESI-TOF): m/z calculated for $C_{25}H_{18}N_4O_4$ requires 461.1220 for $[M+Na]^+$, found 461.1224.

2. Additional Figures

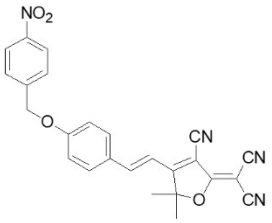

Figure: Full range view of Compound spectra and potential adducts.

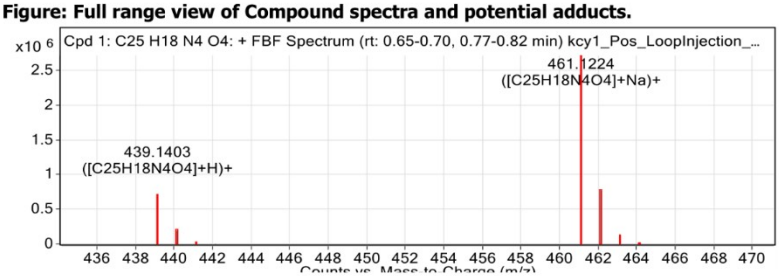

Compound Table

Compound Label	RT (min)	Observed mass (m/z)	Neutral observed mass (Da)	Theoretical mass (Da)	Mass error (ppm)	Isotope match score (%)
Cpd 1: C25 H18 N4 O4	0.73	461.1224	438.1332	438.1328	0.91	99.09

Mass errors of between -5.00 and 5.00 ppm with isotope match scores above 60% are considered confirmation of molecular formulae

Compound isotope peak List

m/z	z	Abund	Formula	Ion
439.1403	1	713251.4	C25H18N4O4	(M+H)+
440.1434	1	192714.4	C25H18N4O4	(M+H)+
441.1476	1	32534.1	C25H18N4O4	(M+H)+
442.1521	1	4759.7	C25H18N4O4	(M+H)+
461.1224	1	2707967.8	C25H18N4O4	(M+Na)+
462.1253	1	770417.4	C25H18N4O4	(M+Na)+
463.1300	1	138692.1	C25H18N4O4	(M+Na)+
464.1336	1	20980.3	C25H18N4O4	(M+Na)+

Figure S1a. The high-resolution mass spectrometry (HRMS) of **TCF-Nitro**.

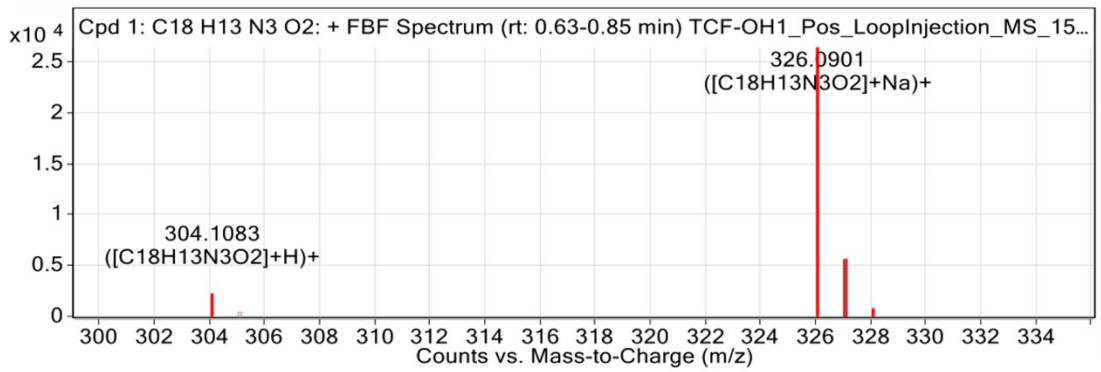

Compound Table

Compound Label	RT (min)	Observed mass (m/z)	Neutral observed mass (Da)	Theoretical mass (Da)	Mass error (ppm)	Isotope match score (%)
Cpd 1: C18 H13 N3 O2	0.74	326.0901	303.1009	303.1008	0.27	85.16

Mass errors of between -5.00 and 5.00 ppm with isotope match scores above 60% are considered confirmation of molecular formulae

Compound isotope peak List

m/z	z	Abund	Formula	Ion
304.1083	1	2195.3	C18H13N3O2	(M+H)+
326.0901	1	26382.3	C18H13N3O2	(M+Na)+
327.0933	1	5475.0	C18H13N3O2	(M+Na)+
328.0942	1	852.0	C18H13N3O2	(M+Na)+

Figure S1b. The high-resolution mass spectrometry (HRMS) after activation with NTR. MS was obtained after 1h reaction of **TCF-Nitro** (10 μM) with 5 μg/mL NTR. The **TCF-OH** ($C_{18}H_{13}N_3O_2$) is observed with mass 303.1009.

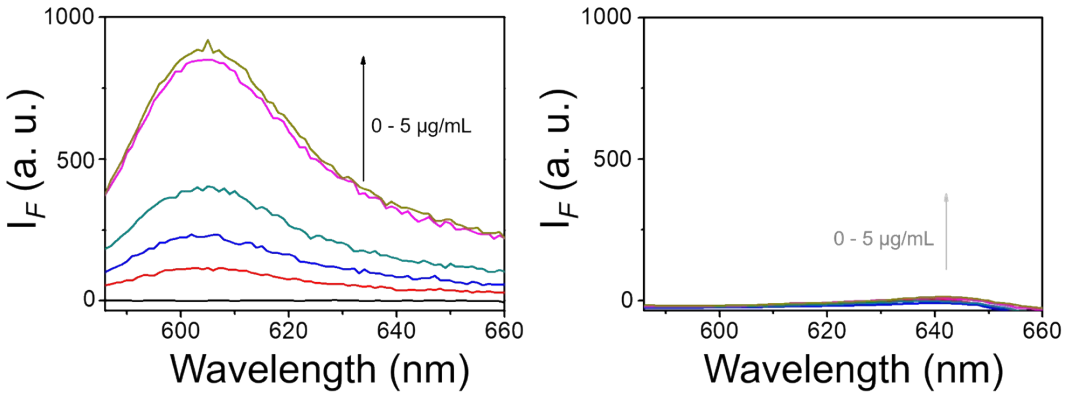

Figure S2. Fluorescence spectra of **TCF-Nitro** (10 μM) in PBS buffer solution (pH = 8.0) with addition of NTR (0 - 5 μg/mL) with (left) or without (right) presence of co-factor NADH (300 μM). λ_{ex} = 560 nm.

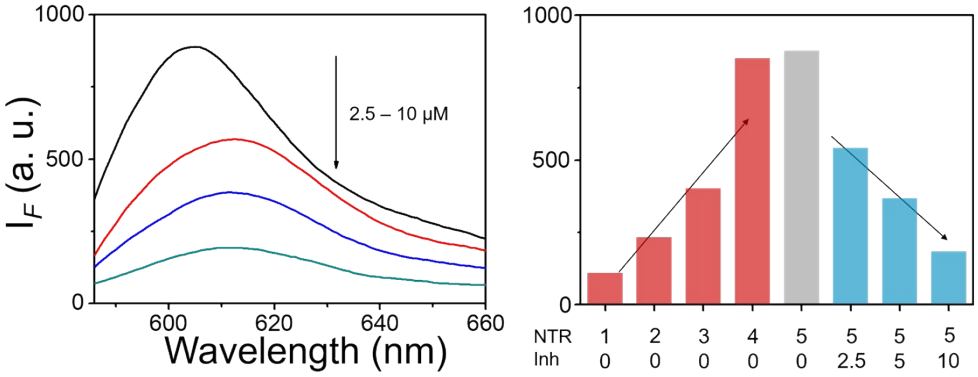

Figure S3. Fluorescence spectra of **TCF-Nitro** (10 μM) in PBS buffer solution (pH = 8.0) with addition of NTR (5 μg/mL) with presence of co-factor NADH (300 μM), with subsequent addition of NTR inhibitor dicoumarin (2.5 – 10 μM) (left). The intensity changes upon NTR activation and the following dicoumarin inhibition (right). λ_{ex} = 560 nm, λ_{em} = 606 nm.

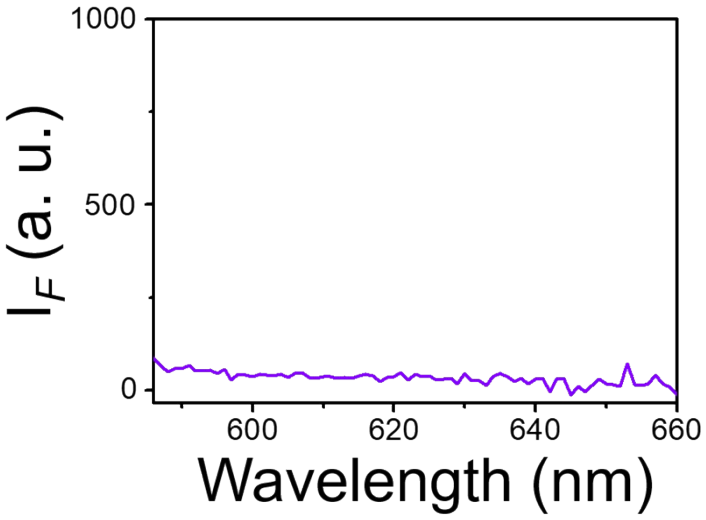

Figure S4. The fluorescence spectrum of dicoumarin (100 μM) under probe detection conditions. λ_{ex} = 560 nm, λ_{em} = 606 nm.

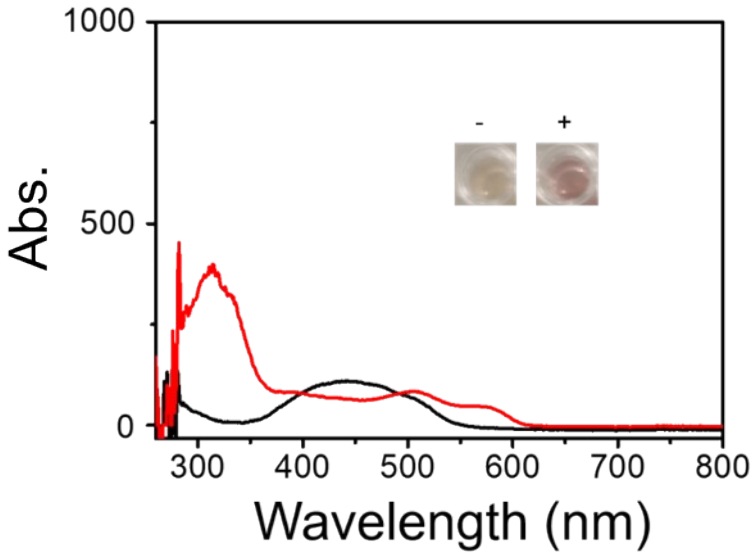

Figure S5. UV-Vis absorption spectrum of **TCF-Nitro** (10 μM) in PBS buffer solution (pH = 8.0) with absence or presence of NTR (5 μg/mL) with co-factor NADH. Photographs representing the color change.

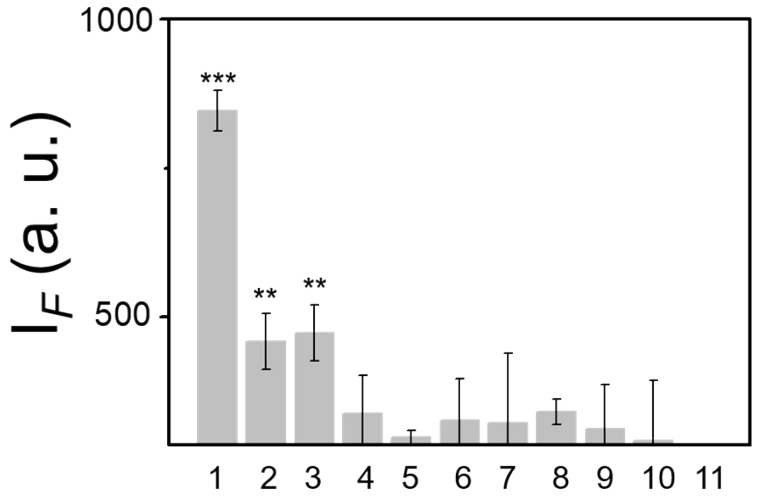

Figure S6. Selectivity on fluorescence response of **TCF-Nitro** over a range of analytes. 1 – NTR (NADH), 2 – NTR, 3 – GSH, 4 – VC (Vitamin C), 5 – H_2O_2, 6 – Met (methionine), 7 – Trp (tryptophan), 8 – Cys (cysteine), 9 – Leu (leucine), 10 – Glu (glucose), 11 – Blank. **P<0.01, ***P<0.001. λ_{ex} = 560 nm, λ_{em} = 606 nm.

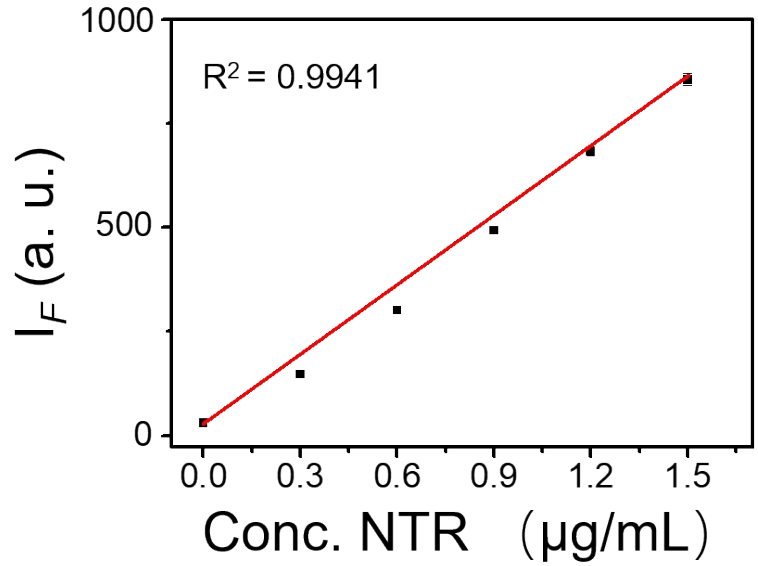

Figure S7. Plotting the linear relationship of fluorescence intensities of **TCF-Nitro** (10 μM) and NTR in low concentrations with co-factor NADH, for determining the limit of detection (LoD). λ_{ex} = 560 nm, λ_{em} = 606 nm.

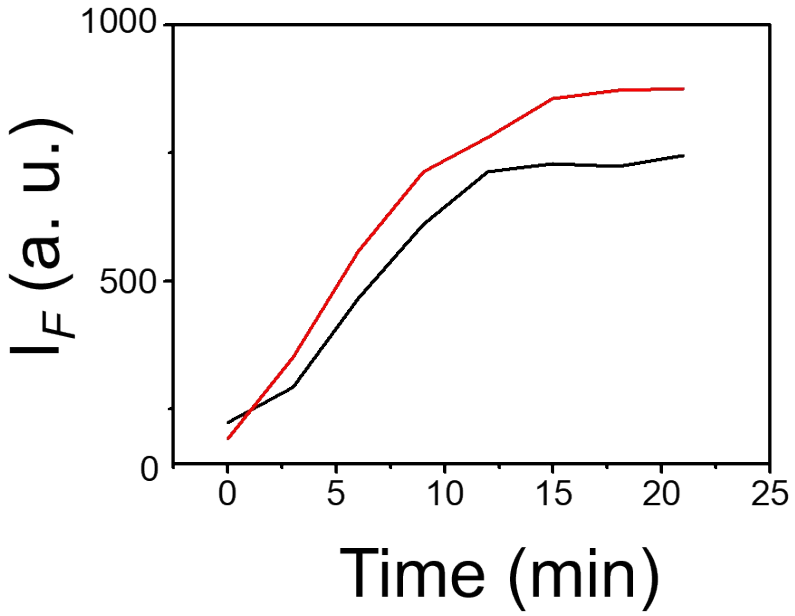

Figure S8. Emission spectroscopic changes along with time for **TCF-Nitro** incubated with 2.5 (black) and 5 μg/mL (red) of NTR with co-factor NADH. λ_{ex} = 560 nm, λ_{em} = 606 nm.

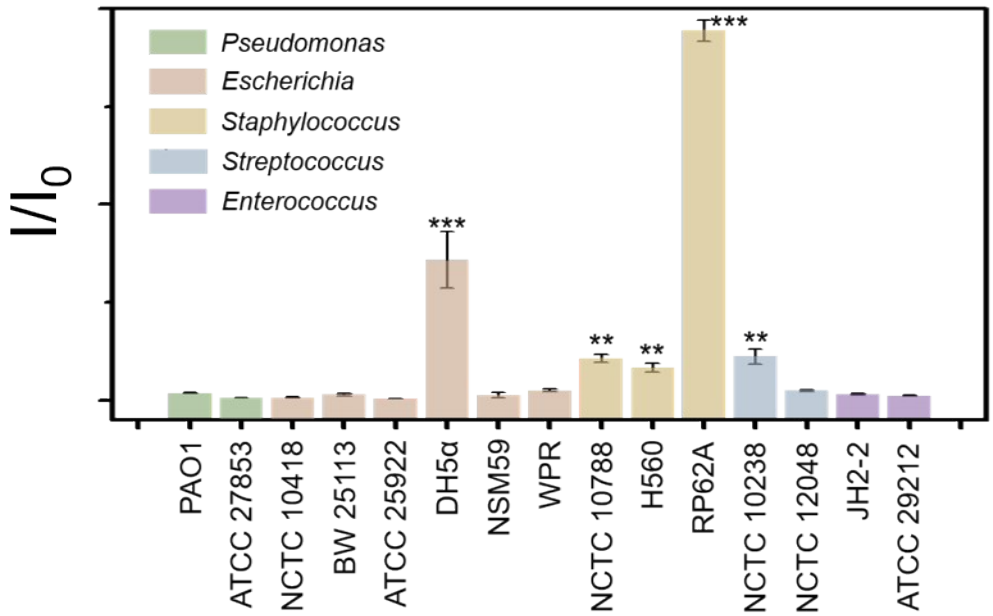

Figure S9. Screening of **TCF-Nitro** NTR activity response among 15 different bacterial species belonging to clinical-prevalent categories *Pseudomonas aeruginosa*, *Escherichia coli*, *Staphylococcus aureus*, *Staphylococcus epidermidis*, *Streptococcus dysgalactiae*, and *Enterococcus faecalis*. **P<0.01, ***P<0.001. λ_{ex} = 560 nm, λ_{em} = 606 nm.

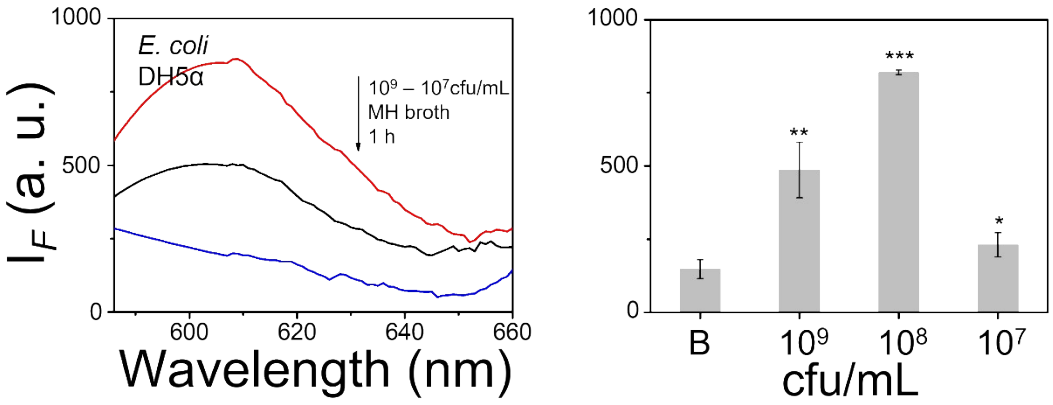

Figure S10. TCF-Nitro based fluorescence detection and corresponding change in fluorescence with 1-100 times diluted MH-cultured *E. coli* DH5α (approx. 10^9 cfu/mL) to determine NTR activity and probe detection limits, under 1 h detection time. *P<0.1, **P<0.01, ***P<0.001. λ_{ex} = 560 nm, λ_{em} = 606 nm.

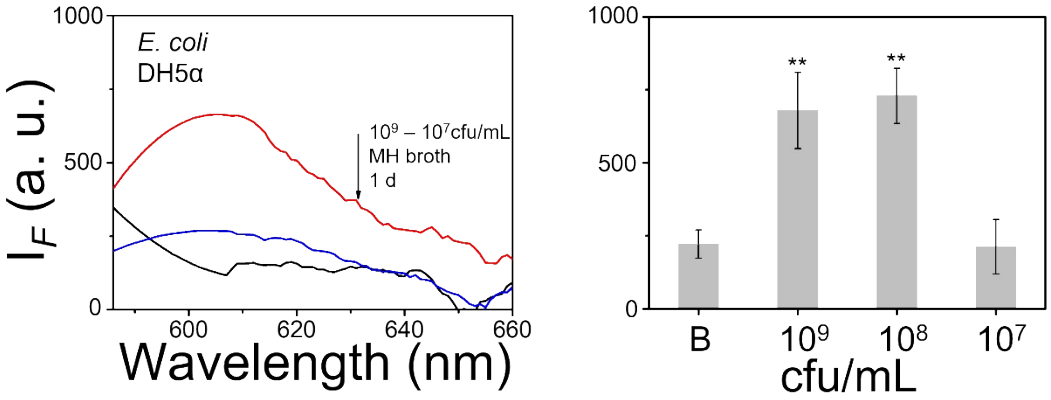

Figure S11. TCF-Nitro based fluorescence detection and corresponding change in fluorescence with 1-100 times diluted MH-cultured *E. coli* DH5α (approx. 10^9 cfu/mL) to determine NTR activity and probe detection limits, under 1 d detection time. **P<0.01. λ_{ex} = 560 nm, λ_{em} = 606 nm.

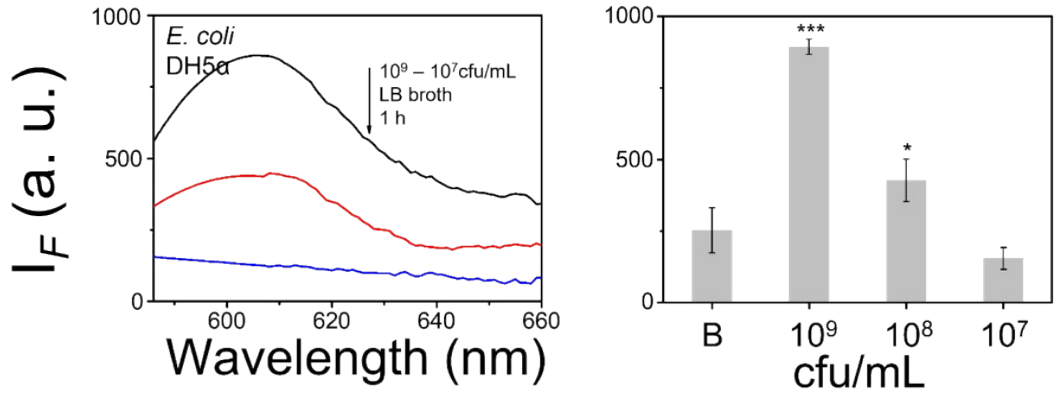

Figure S12. TCF-Nitro based fluorescence detection and corresponding change in fluorescence with 1-100 times diluted LB-cultured *E. coli* DH5α (approx. 10^9 cfu/mL) to determine NTR activity and probe detection limits, under 1 h detection time. *P<0.1, ***P<0.001. λ_{ex} = 560 nm, λ_{em} = 606 nm.

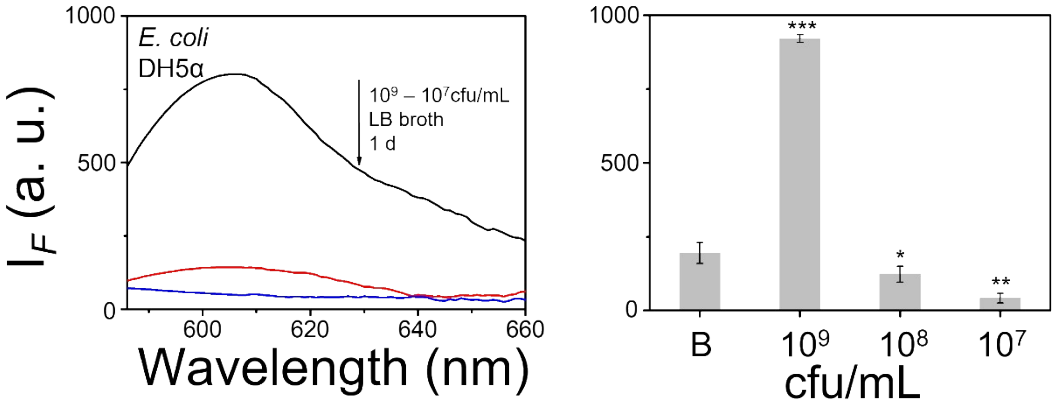

Figure S13. TCF-Nitro based fluorescence detection and corresponding change in fluorescence with 1-100 times diluted LB-cultured *E. coli* DH5α (approx. 10^9 cfu/mL) to determine NTR activity and probe detection limits, under 1 d detection time. *P<0.1, **P<0.01, ***P<0.001. λ_{ex} = 560 nm, λ_{em} = 606 nm.

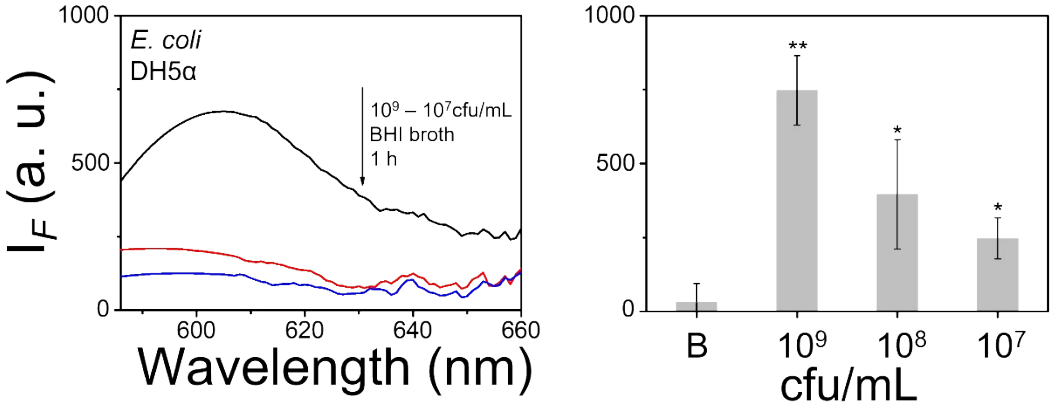

Figure S14. TCF-Nitro based fluorescence detection and corresponding change in fluorescence with 1-100 times diluted BHI-cultured *E. coli* DH5α (approx. 10^9 cfu/mL) to determine NTR activity and probe detection limits, under 1 h detection time. *P<0.1, **P<0.01. λ_{ex} = 560 nm, λ_{em} = 606 nm.

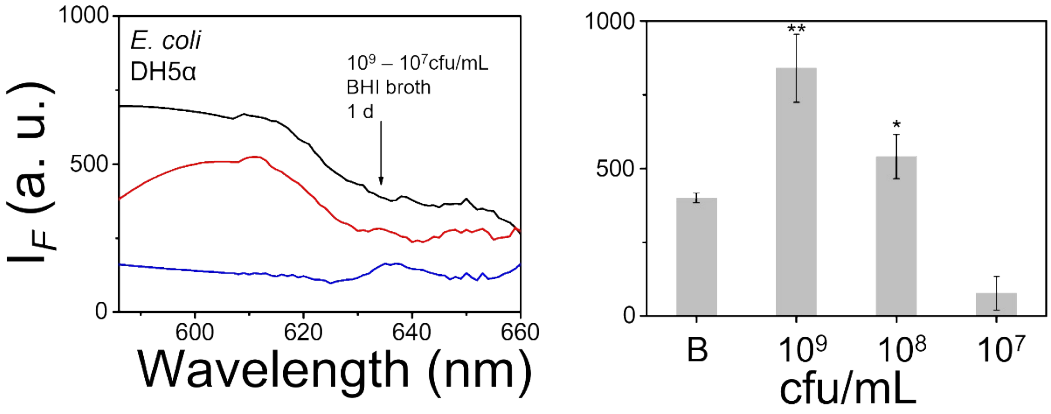

Figure S15. TCF-Nitro based fluorescence detection and corresponding change in fluorescence with 1-100 times diluted BHI-cultured *E. coli* DH5α (approx. 10^9 cfu/mL) to determine NTR activity and probe detection limits, under 1 d detection time. *P<0.1, **P<0.01. λ_{ex} = 560 nm, λ_{em} = 606 nm.

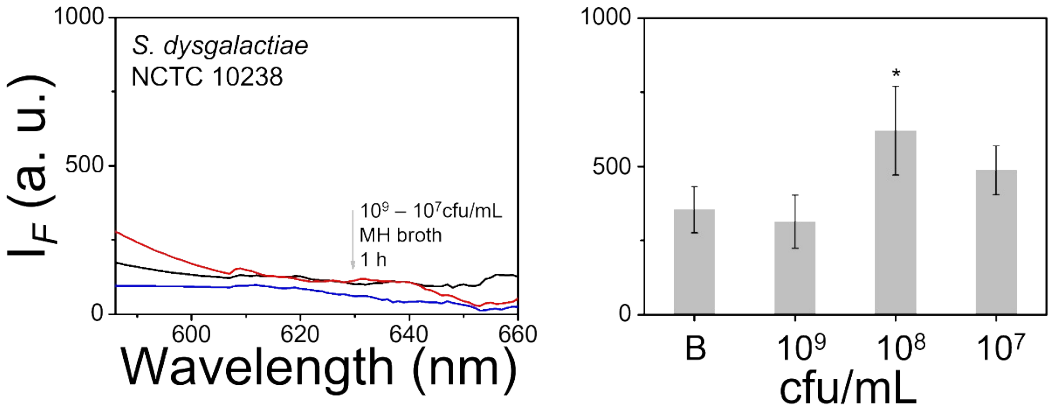

Figure S16. TCF-Nitro based fluorescence detection and corresponding change in fluorescence with 1-100 times diluted MH-cultured *S. dysgalactiae* NCTC 10238 (approx. 10^9 cfu/mL) to determine NTR activity and probe detection limits, under 1 h detection time. *P<0.1. λ_{ex} = 560 nm, λ_{em} = 606 nm.

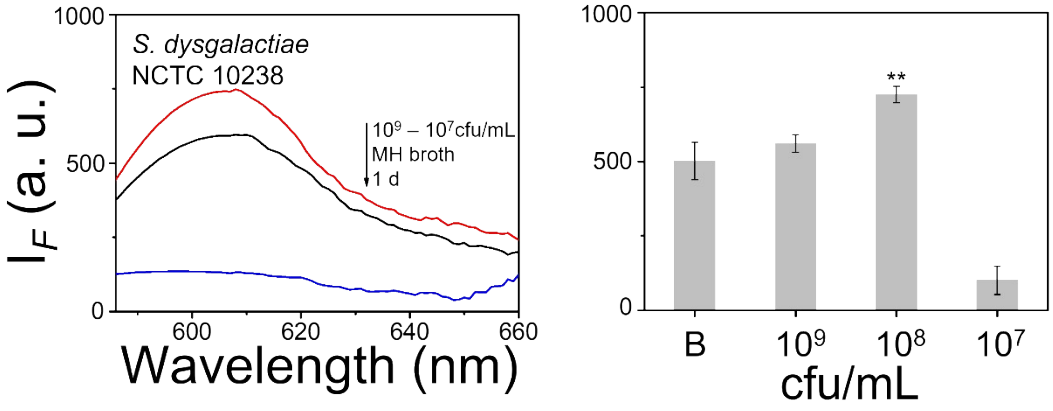

Figure S17. TCF-Nitro based fluorescence detection and corresponding change in fluorescence with 1-100 times diluted MH-cultured *S. dysgalactiae* NCTC 10238 (approx. 10^9 cfu/mL) to determine NTR activity and probe detection limits, under 1 d detection time. **P<0.01. λ_{ex} = 560 nm, λ_{em} = 606 nm.

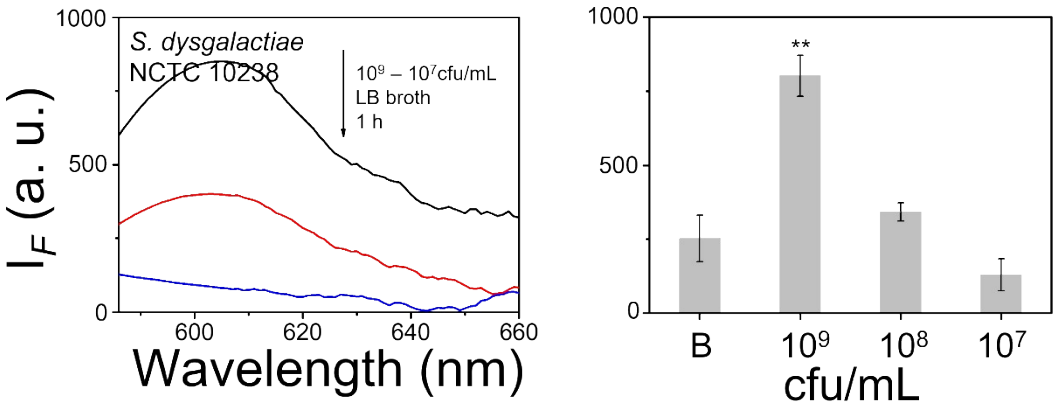

Figure S18. TCF-Nitro based fluorescence detection and corresponding change in fluorescence with 1-100 times diluted LB-cultured *S. dysgalactiae* NCTC 10238 (approx. 10^9 cfu/mL) to determine NTR activity and probe detection limits, under 1 h detection time. **P<0.01. λ_{ex} = 560 nm, λ_{em} = 606 nm.

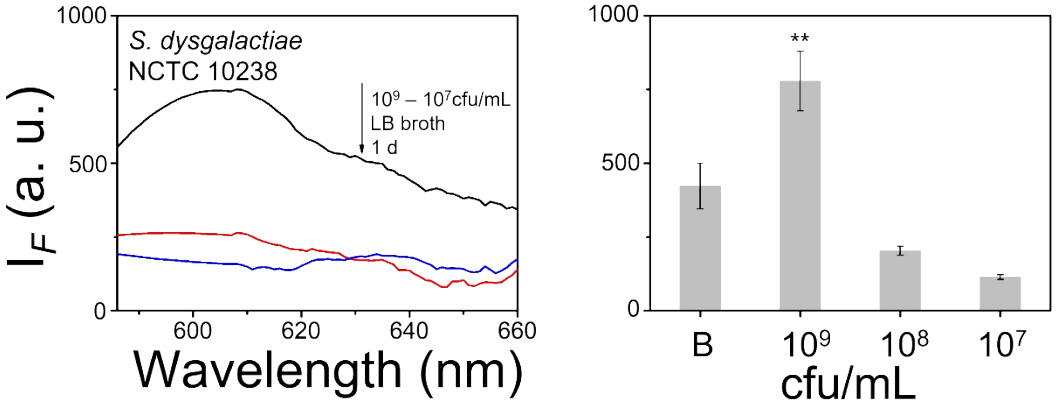

Figure S19. TCF-Nitro based fluorescence detection and corresponding change in fluorescence with 1-100 times diluted LB-cultured *S. dysgalactiae* NCTC 10238 (approx. 10^9 cfu/mL) to determine NTR activity and probe detection limits, under 1 d detection time. **P<0.01. λ_{ex} = 560 nm, λ_{em} = 606 nm.

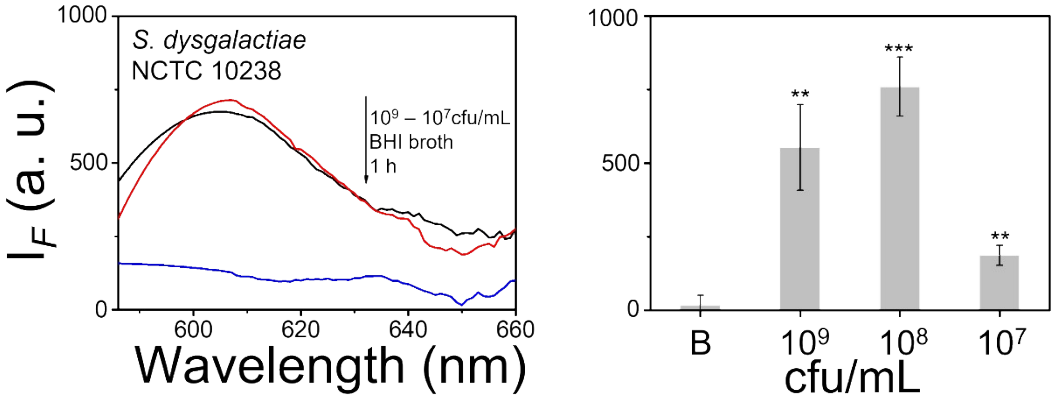

Figure S20. TCF-Nitro based fluorescence detection and corresponding change in fluorescence with 1-100 times diluted BHI-cultured *S. dysgalactiae* NCTC 10238 (approx. 10^9 cfu/mL) to determine NTR activity and probe detection limits, under 1 h detection time. **P<0.01, ***P<0.001. λ_{ex} = 560 nm, λ_{em} = 606 nm.

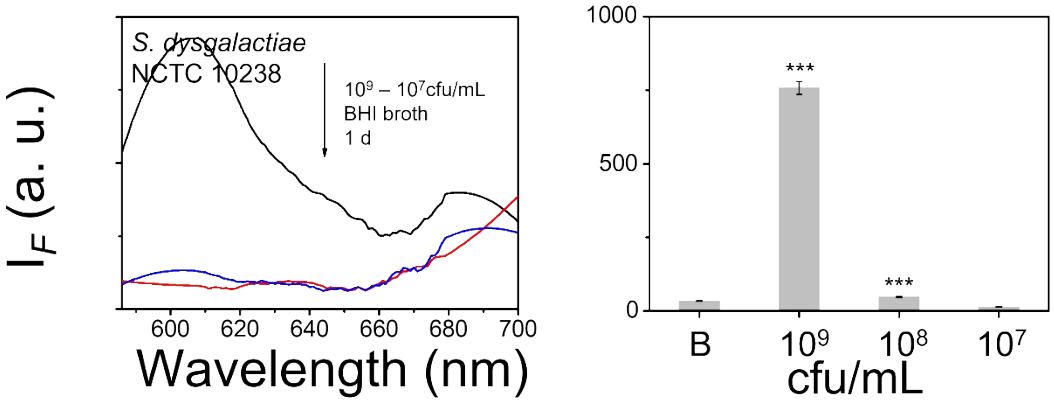

Figure S21. TCF-Nitro based fluorescence detection and corresponding change in fluorescence with 1-100 times diluted BHI-cultured *S. dysgalactiae* NCTC 10238 (approx. 10^9 cfu/mL) to determine NTR activity and probe detection limits, under 1 d detection time. ***P<0.001. λ_{ex} = 560 nm, λ_{em} = 606 nm.

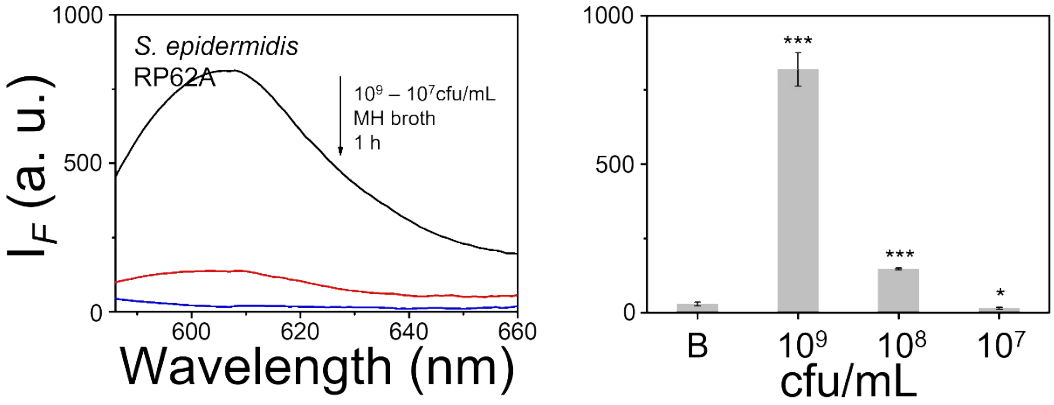

Figure S22. TCF-Nitro based fluorescence detection and corresponding change in fluorescence with 1-100 times diluted MH-cultured *S. epidemidis* RP62A (approx. 10^9 cfu/mL) to determine NTR activity and probe detection limits, under 1 h detection time. *P<0.1, ***P<0.001. λ_{ex} = 560 nm, λ_{em} = 606 nm.

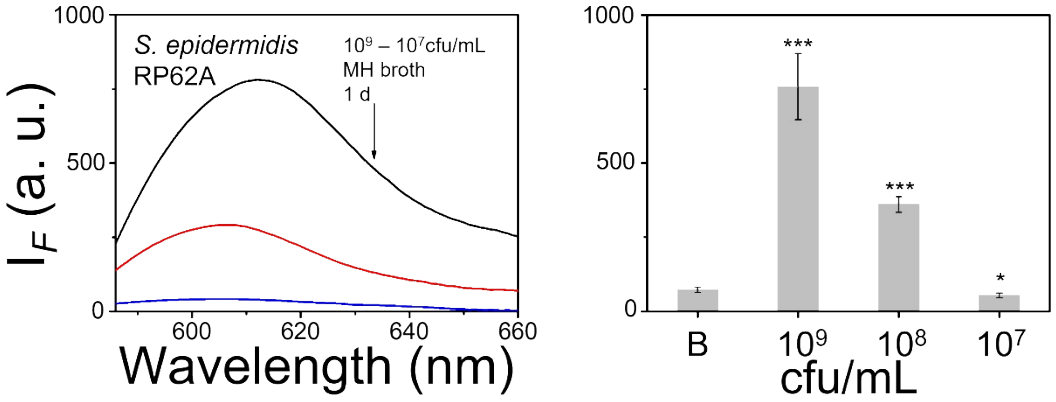

Figure S23. TCF-Nitro based fluorescence detection and corresponding change in fluorescence with 1-100 times diluted MH-cultured *S. epidemidis* RP62A (approx. 10^9 cfu/mL) to determine NTR activity and probe detection limits, under 1 d detection time. *P<0.1, ***P<0.001. λ_{ex} = 560 nm, λ_{em} = 606 nm.

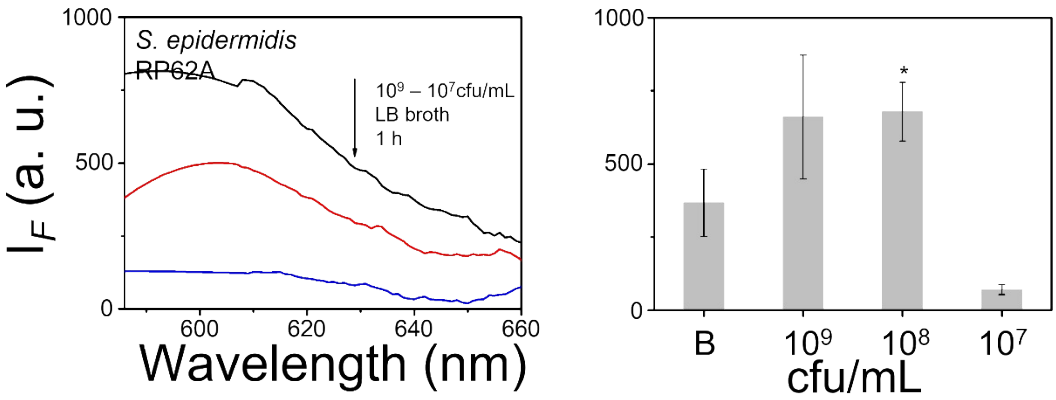

Figure S24. TCF-Nitro based fluorescence detection and corresponding change in fluorescence with 1-100 times diluted LB-cultured *S. epidemidis* RP62A (approx. 10^9 cfu/mL) to determine NTR activity and probe detection limits, under 1 h detection time. *P<0.1. λ_{ex} = 560 nm, λ_{em} = 606 nm.

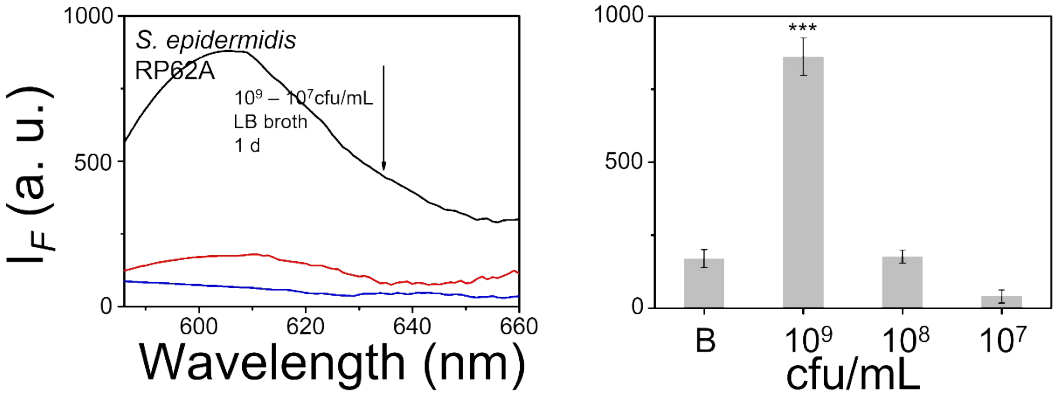

Figure S25. TCF-Nitro based fluorescence detection and corresponding change in fluorescence with 1-100 times diluted LB-cultured *S. epidemidis* RP62A (approx. 10^9 cfu/mL) to determine NTR activity and probe detection limits, under 1 d detection time. ***P<0.001. λ_{ex} = 560 nm, λ_{em} = 606 nm.

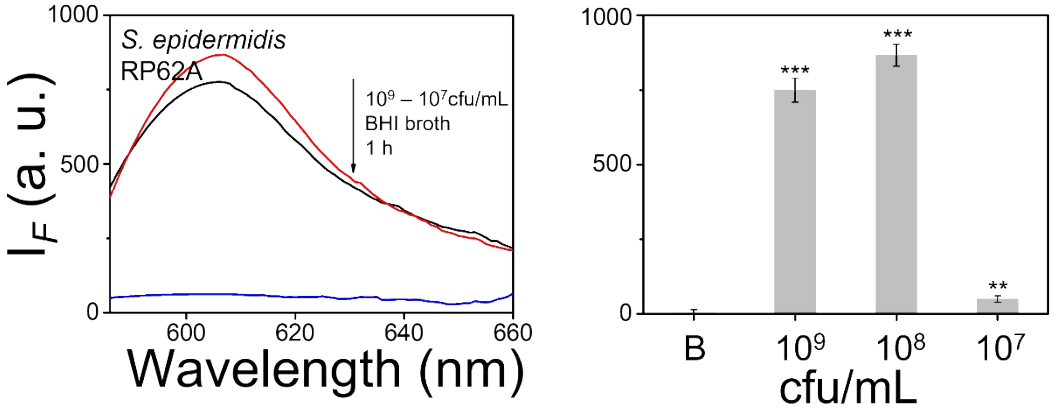

Figure S26. TCF-Nitro based fluorescence detection and corresponding change in fluorescence with 1-100 times diluted BHI-cultured *S. epidemidis* RP62A (approx. 10^9 cfu/mL) to determine NTR activity and probe detection limits, under 1 h detection time. **P<0.01, ***P<0.001. λ_{ex} = 560 nm, λ_{em} = 606 nm.

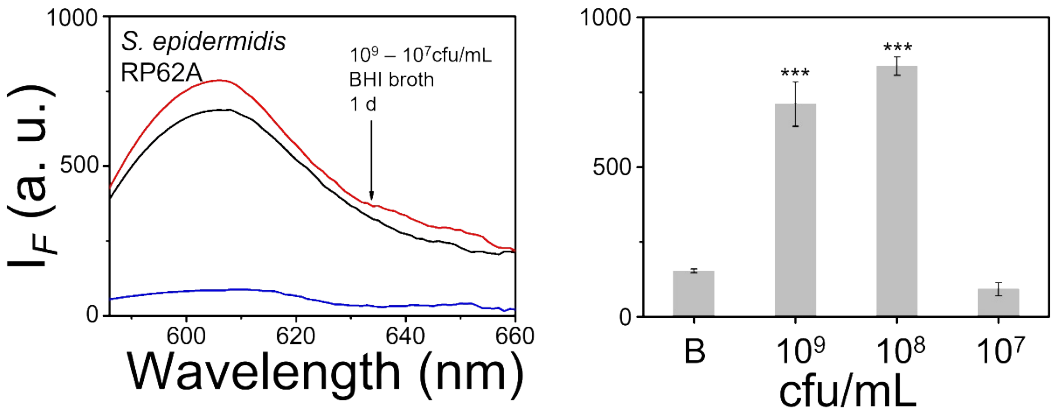

Figure S27. TCF-Nitro based fluorescence detection and corresponding change in fluorescence with 1-100 times diluted BHI-cultured *S. epidemidis* RP62A (approx. 10^9 cfu/mL) to determine NTR activity and probe detection limits, under 1 d detection time. ***P<0.001. λ_{ex} = 560 nm, λ_{em} = 606 nm.

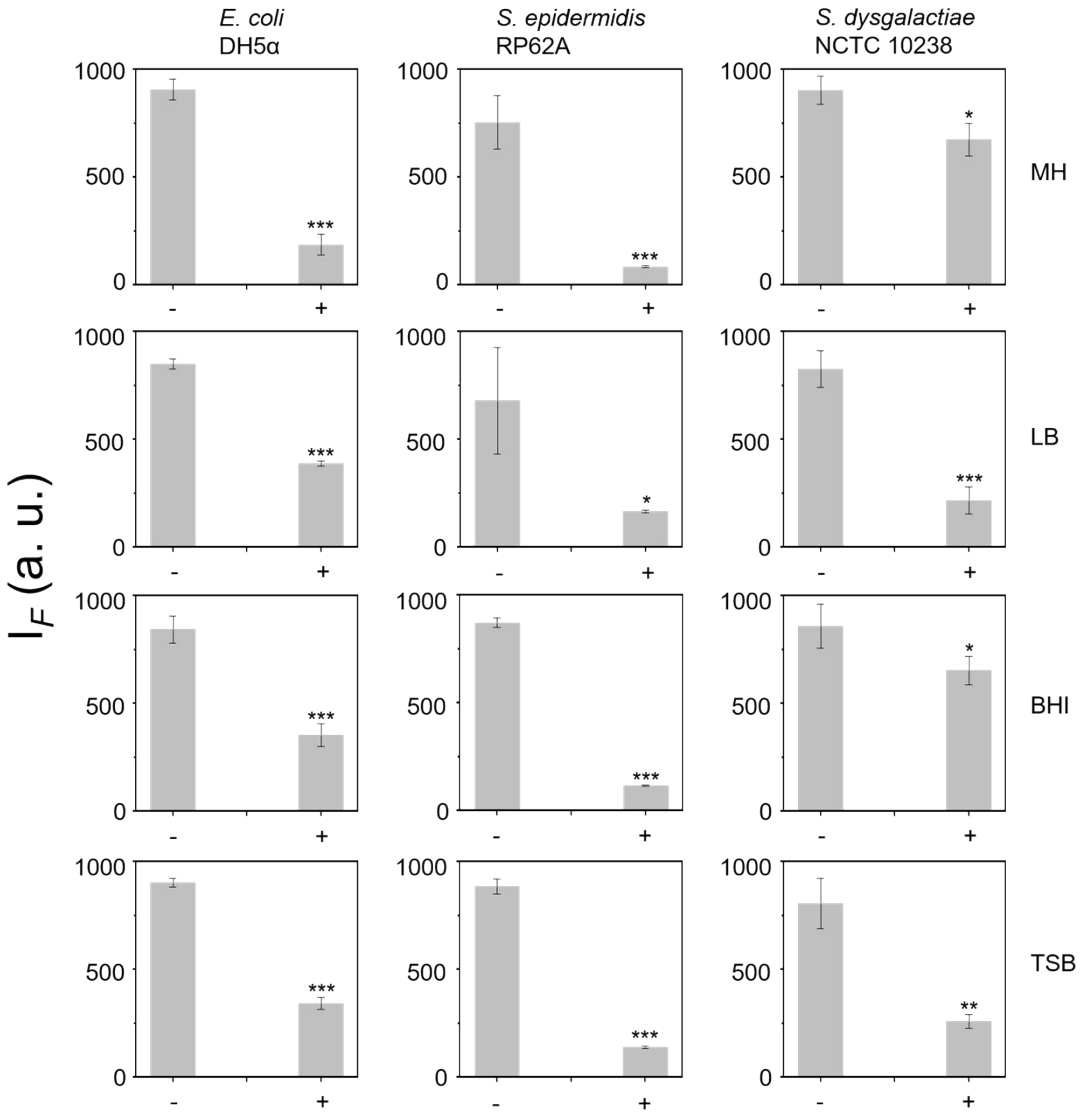

Figure S28. The corresponding change in fluorescence of **TCF-Nitro** treated *E. coli* DH5α, *S. dysgalactiae* NCTC 10238, and *S. epidemidis* RP62A, without (-) or with (+) presence of NTR inhibitor dicoumarin. *P<0.1, **P<0.01, ***P<0.001. λ_{ex} = 560 nm, λ_{em} = 606 nm.

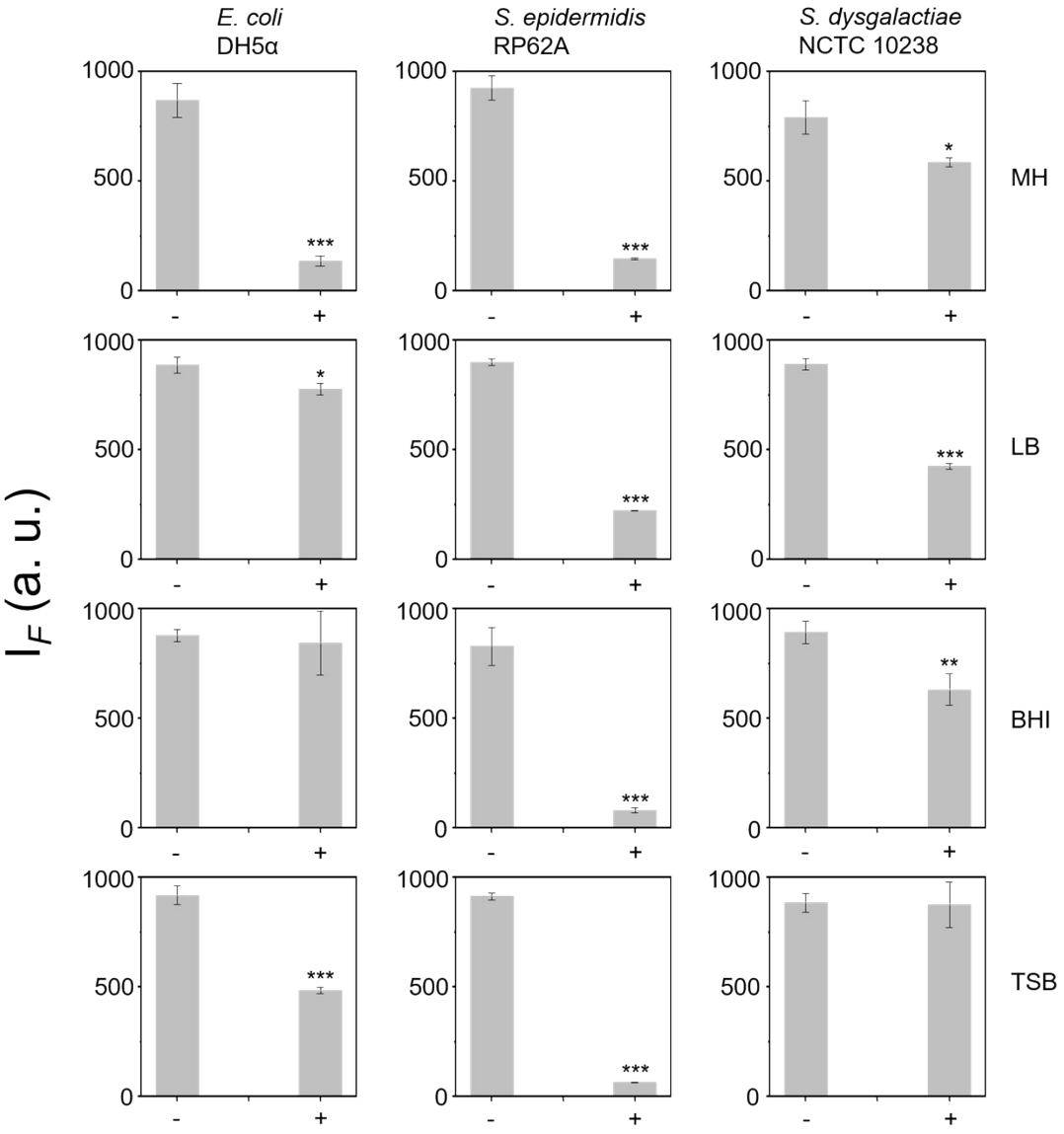

Figure S29. The corresponding change in fluorescence of **TCF-Nitro** treated *E. coli* DH5α, *S. dysgalactiae* NCTC 10238, and *S. epidemidis* RP62A, without (-) presence of NTR inhibitor dicoumarin, or with the pre-treatment of inhibitor then washed out before incubating probe (+). *P<0.1, **P<0.01, ***P<0.001. λ_{ex} = 560 nm, λ_{em} = 606 nm.

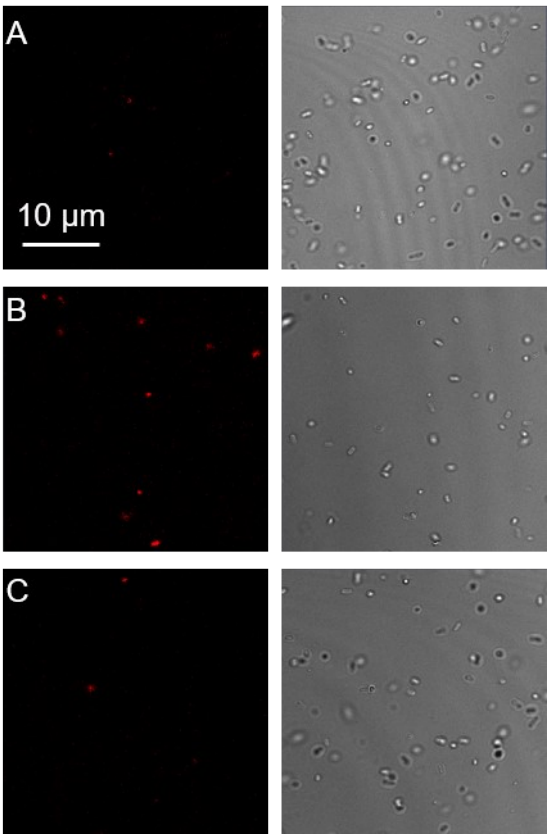

Figure S30. Confocal Laser-Scanning Microscopy (CLSM) imaging of the intracellular signal of **TCF-Nitro**-stained *E. coli* DH5α with or without presence of NTR inhibitor dicoumarin. A – control, B – stained cells without inhibitor, C – stain cells with inhibitor. λ_{ex} = 561 nm (laser source), λ_{em} = 606 nm.

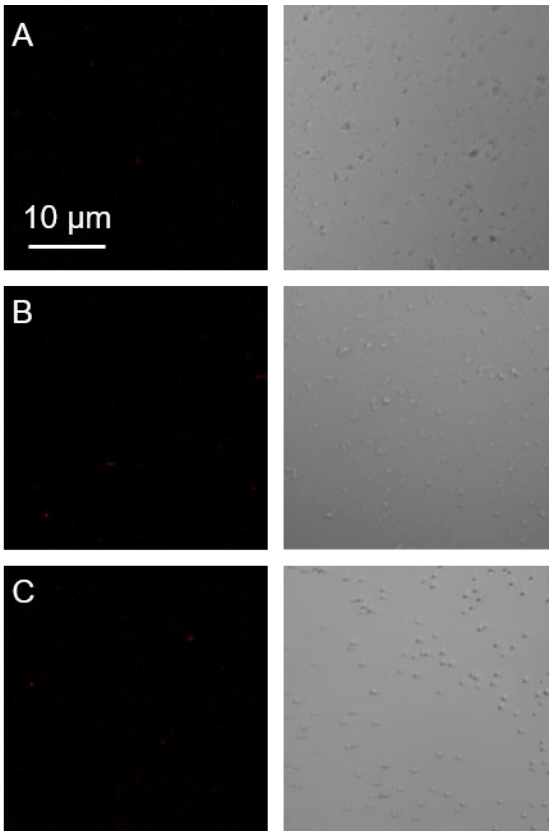

Figure S31. Confocal Laser-Scanning Microscopy (CLSM) imaging of the intracellular signal of **TCF-Nitro**-stained *S. epidemidis* RP62A with or without presence of NTR inhibitor dicoumarin. A – control, B – stained cells without inhibitor, C – stain cells with inhibitor. λ_{ex} = 561 nm (laser source), λ_{em} = 606 nm.

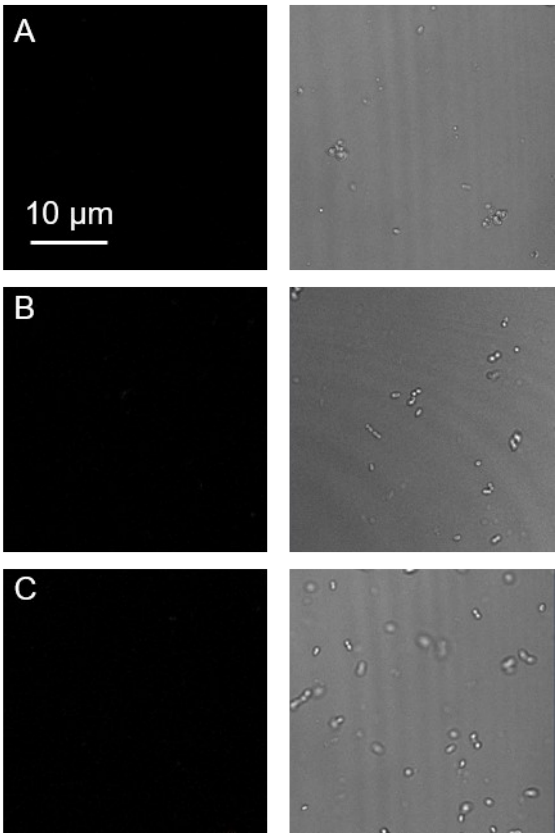

Figure S32. Confocal Laser-Scanning Microscopy (CLSM) imaging of the intracellular signal of **TCF-Nitro**-stained *S. dysgalactiae* NCTC 10238 with or without presence of NTR inhibitor dicoumarin. A – control, B – stained cells without inhibitor, C – stain cells with inhibitor. λ_{ex} = 561 nm (laser source), λ_{em} = 606 nm.

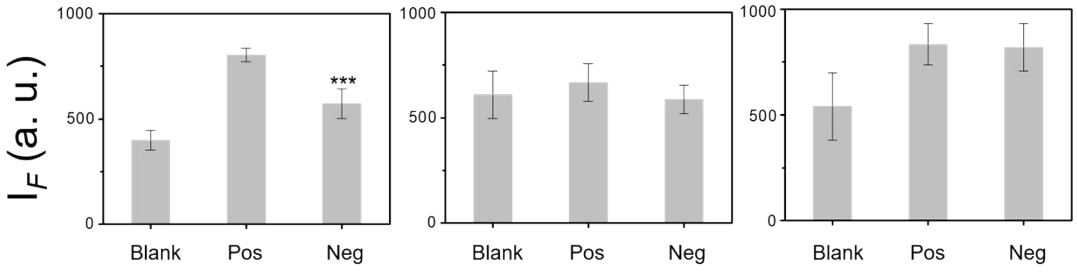

Figure S33. Quantitative fluorescence intensities of the images in Figure S29 – Figure S31. Pos - stained cells without inhibitor, Neg - stain cells with inhibitor. From left to right: *E. coli* DH5α, *S. epidemidis* RP62A, *S. dysgalactiae* NCTC 10238. ***P<0.001. λ_{ex} = 561 nm (laser source), λ_{em} = 606 nm.

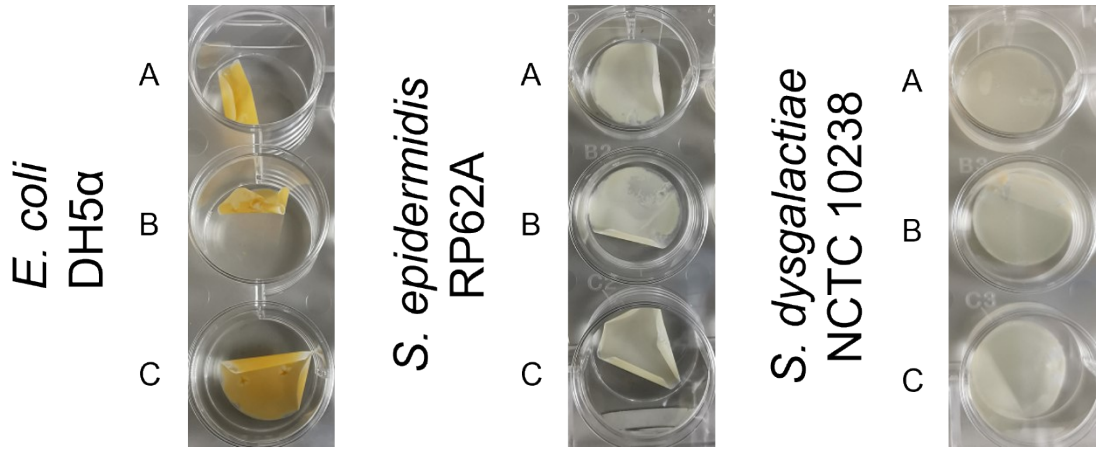

Figure S34. Colony biofilms of *E. coli* DH5α, *S. epidermidis* RP62A, and *S. dysgalactiae* NCTC 10238 on polycarbonate membrane before treatment.

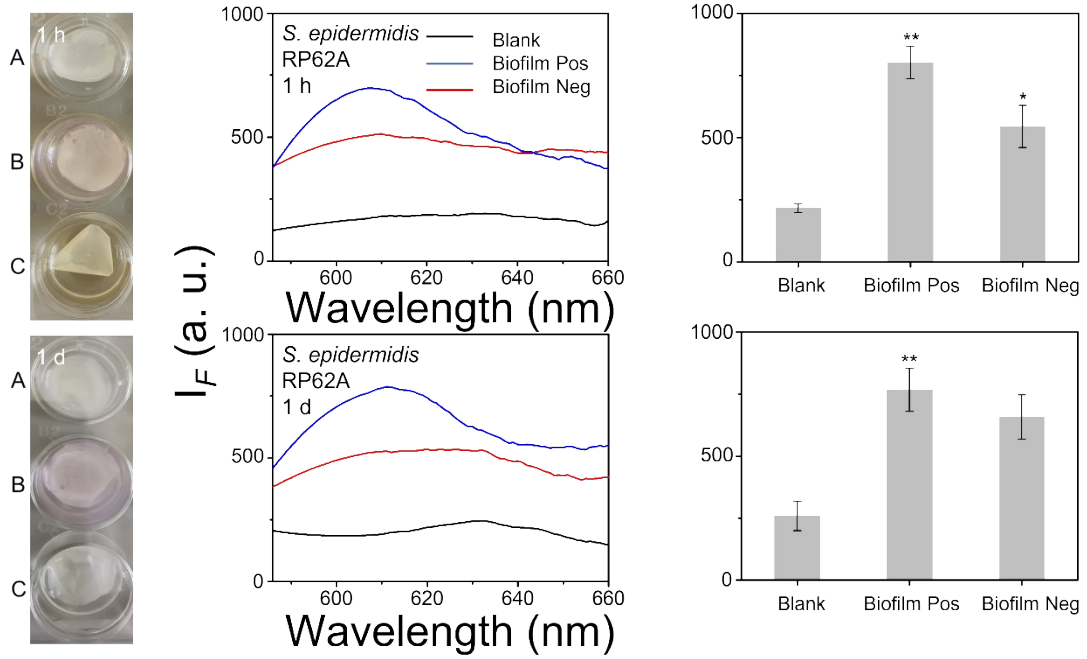

Figure S35. Images taken of negative controls (biofilms on membrane and Artificial Wound Fluid (AWF) only) (A) and biofilms of *S. epidermidis* RP62A after incubation with 10 μM **TCF-Nitro** in PBS buffer pH = 8.0 at 37 °C without (B) or with (C) further treatment of inhibitor dicoumarin, for 1 h and 1 d respectively (left). Fluorescence spectrum performances and corresponding change in fluorescence for the wells of colony biofilms on the left (right). Biofilm Pos means biofilms after incubation with 10 μM **TCF-Nitro** in PBS buffer pH = 8.0 at 37 °C without inhibitor. Biofilm Neg means biofilms after incubation with 10 μM **TCF-Nitro** in PBS buffer pH = 8.0 at 37 °C with inhibitor. *P<0.1, **P<0.01. λ_{ex} = 560 nm, λ_{em} = 606 nm.

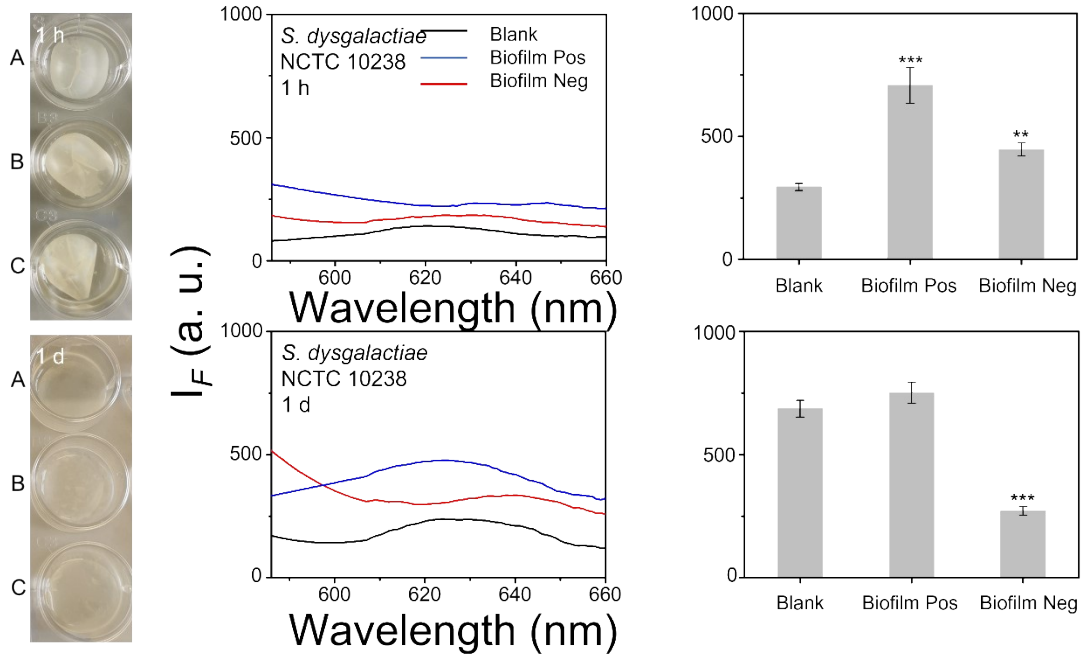

Figure S36. Images taken of negative controls (biofilms on membrane and Artificial Wound Fluid (AWF) only) (A) and biofilms of *S. dysgalactiae* NCTC 10238 after incubation with 10 µM **TCF-Nitro** in PBS buffer pH = 8.0 at 37 °C without (B) or with (C) further treatment of inhibitor dicoumarin, for 1 h and 1 d respectively (left). Fluorescence spectrum performances and corresponding change in fluorescence for the wells of colony biofilms on the left (right). Biofilm Pos means biofilms after incubation with 10 µM **TCF-Nitro** in PBS buffer pH = 8.0 at 37 °C without inhibitor. Biofilm Neg means biofilms after incubation with 10 µM **TCF-Nitro** in PBS buffer pH = 8.0 at 37 °C with inhibitor. **P<0.01, ***P<0.001. λ_{ex} = 560 nm, λ_{em} = 606 nm.

3. Spectral Copies

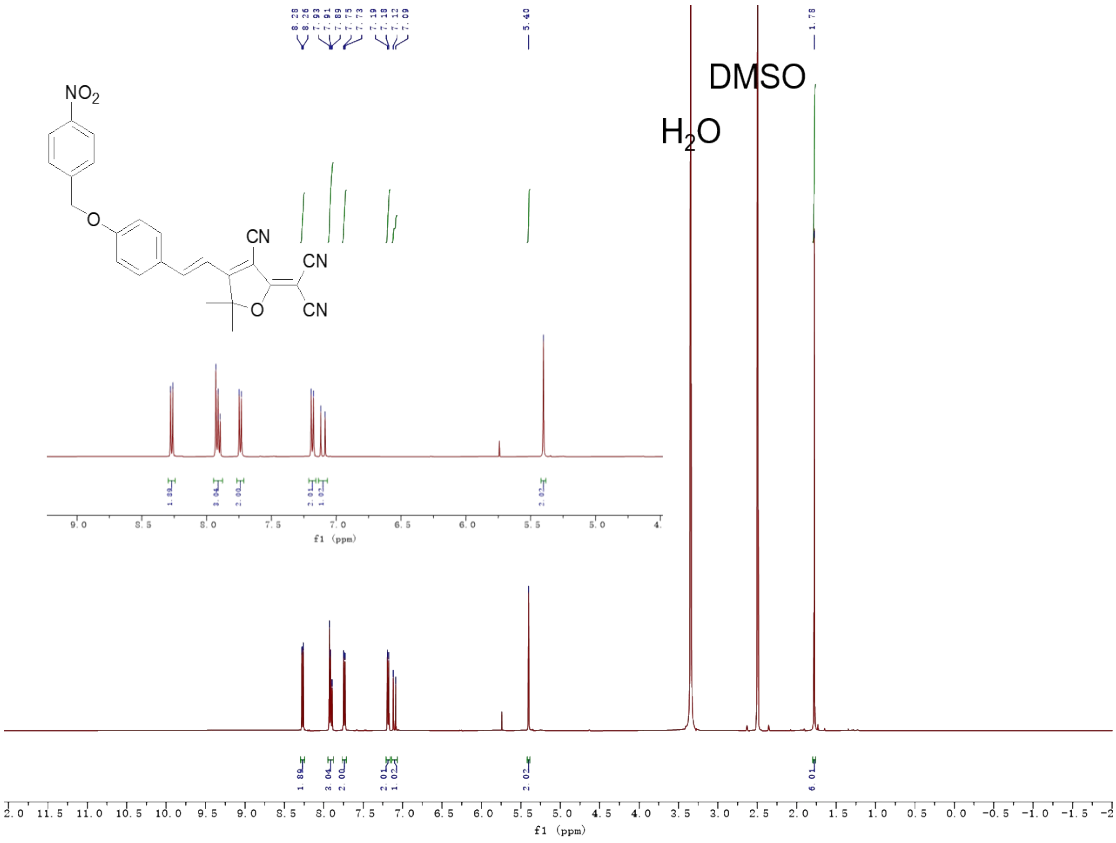

Figure S37. ^{1}H NMR of **TCF-Nitro**.

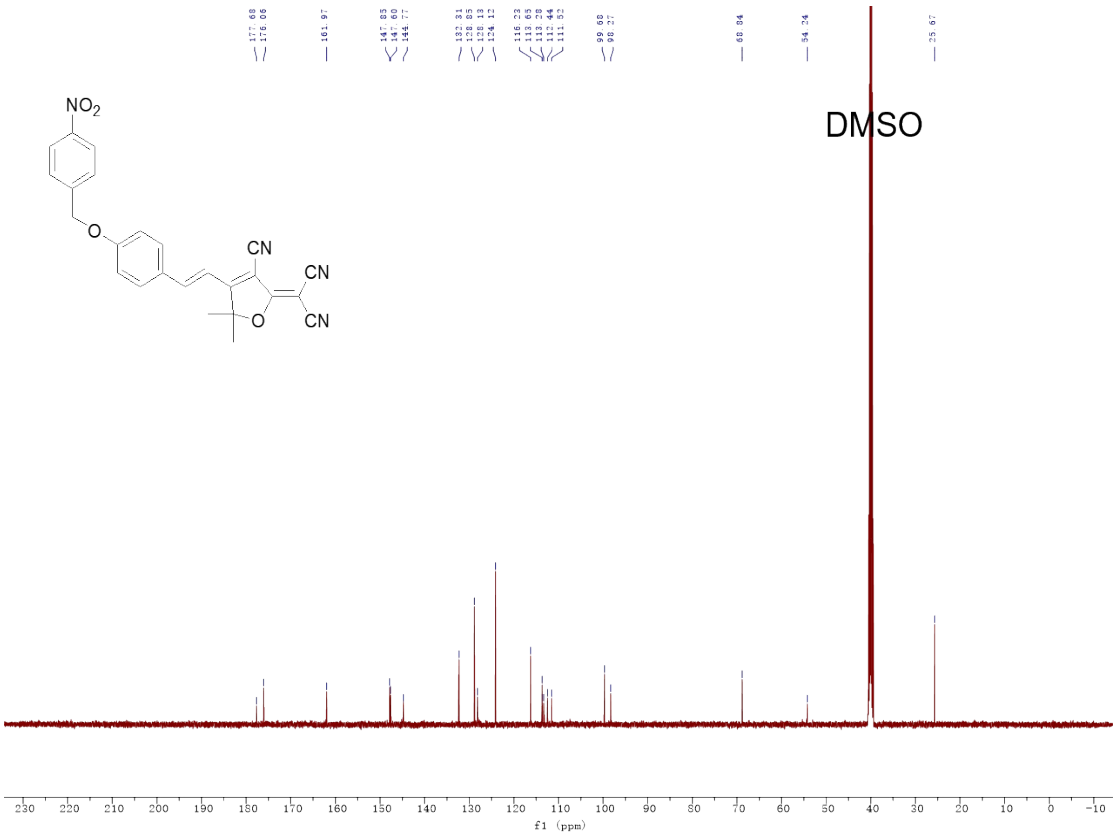

Figure S38. ^{13}C NMR of **TCF-Nitro**.

4. Additional References

1. N. T. Thet, D. R. Alves, J. E. Bean, S. Booth, J. Nzakizwanayo, A. E. R. Young, B. V. Jones, A. T. A. Jenkins. *ACS Appl. Mater. Interfaces*., **2016**, *8*, 14909.
2. A. C. Sedgwick, H.-H. Han, J. E. Gardiner, S. D. Bull, X.-P. He, T. D. James. *Chem. Commun.*, **2017**, *53*, 12822.